24th INTERNATIONAL CONGRESS ON SOUND AND VIBRATION
23–27 July 2017, London

A COMPARATIVE STUDY OF GRAVITATIONAL ACCELERATION CANCELLATION FROM ON-ROTOR MEMS ACCELEROMETERS FOR CONDITION MONITORING

Mones Z., Feng G., Tang X., Haba U., Gu F. and Ball A. D.

University of Huddersfield, Queensgate, Huddersfield, HD1 3DH, UK,

email: Zainab.Mones@hud.ac.uk

Abstract: there have recently been significant enhancements in Micro-Electro-Mechanical Systems (MEMS) technologies, which have provided an easier and cheaper means of condition monitoring for rotating machines by installing MEMS accelerometers directly onto rotors. One critical issue in using on-rotor MEMS accelerometers is extracting the real tangential acceleration from accelerometer outputs which also contain gravitational acceleration. This paper studies and compares two different methods that can be used to eliminate the gravitational acceleration so as to characterise the rotor dynamics precisely. In the first method, the pure tangential acceleration is reconstructed by combining two orthogonal outputs of a single MEMS accelerometer attached to the rotating part. The second method uses two MEMS accelerometers mounted diametrically opposite each other on the reciprocating compressor flywheel, allowing the gravitational acceleration signal to be cancelled by summing the acceleration signals from both sensors. Based on analytical and experimental results, gravitational acceleration can be successfully eliminated by both methods, and the calculated tangential acceleration signal can effectively reflect the running status of a reciprocating compressor subject to the leakage fault.

Keywords: MEMS, on-rotor measurement, condition monitoring.

1. Introduction

Recent years have witnessed incredible developments in Micro Electro Mechanical Systems (MEMS), which provide a cost-effective way of monitoring rotor vibration by installing MEMS accelerometers directly onto the rotating components of machines. MEMS sensors are typically low-cost, low-power and small devices, some of which have capabilities to not only process the acquired data, but also send it using wireless communication [1],[2]. Many studies have explored the usage of MEMS accelerometers in the condition monitoring field. For example, Arebi et al. investigated the performance of different accelerometers used for misalignment detection [3]. They compared the response from various data acquired via a wireless MEMS accelerometer, a laser vibrometer, shaft encoder and an accelerometer under various degrees of shaft misalignment. Their study concluded that the wireless MEMS accelerometer outperforms the other sensors and produces a full classification of different misalignment levels, as well as showing a unique increasing trend with speed [3]. In [4], the authors mounted a MEMS accelerometer on an induction motor to acquire vibration signals which can be used for condition monitoring. This study concluded that different mechanical and electrical fault conditions of the induction motor could be easily detected and characterised by analysing the vibration spectrum. Elnady et al. [5] installed a low-weight MEMS accelerometer and a wireless sensor node directly onto a shaft to study the critical speed during machine run-up, and Thompson [6] employed a high-range but low sensitivity MEMS accelerometer to acquire the centrifugal acceleration of a fan blade.

Feng et al. [7] attached AX3, a three-axial MEMS data logger, onto a reciprocating compressor flywheel to measure on-rotor acceleration signals that can be used to monitor compressor

performance. Later, Mones et al. developed the work implemented in [7], improving on the data collection method by using BLE protocol instead of data logging and thus allowing the system to become online condition monitoring [8].

One of the most critical issues in using on-rotor MEMS accelerometers for condition monitoring is removing gravitational acceleration from the MEMS outputs. The main target of this paper is therefore to study how gravitational acceleration can be eliminated from MEMS sensor outputs so that the tangential acceleration, which characterises the rotor dynamics, can be obtained and used to monitor the condition of a reciprocating compressor.

2. Theoretical background

The MEMS accelerometer is an electromechanical device that measures absolute acceleration force, which means it measures rotor dynamic information as well as the effects of earth gravity [9]. Figure 1 shows the rotating movement of a MEMS sensor around the centre O, as well as acceleration components on both the X-axis and Y-axis. Detailed information about the acceleration signals of a rotating mass can be found in [7].

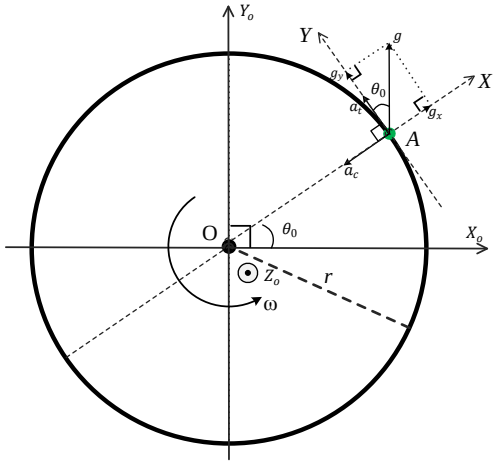

Figure 1: Acceleration analysis of a mass M rotating around point O

When sensor A rotates around O, the gravity acceleration will project onto the X- and Y-axes of the sensor. Therefore, the outputs of the sensor can be calculated as:

$$\begin{aligned} a_x &= -a_c + g_x = -a_c + g\sin\theta \\ a_y &= a_t + g_y = a_t + g\cos\theta \end{aligned} \tag{1}$$

According to [7], the approximate output on the Y-axis, which implements a compound signal containing both tangential acceleration and gravitational acceleration projections, can be expressed as:

$$\tilde{a}_y \approx \sum_{n=1}^{\infty} nr\omega_0 A_n \cos\left(n\omega_0 t + \varphi_n\right) - g\cos\theta_0 \tag{2}$$

where ω_0 represents the steady angular speed while A_n and φ_n represent the amplitude and phase of the n^{th} component in $\tilde{a}_y$ respectively.

Based on Equation 2, both gravitational acceleration and tangential acceleration can be drawn in the time and frequency domain. From Figure 2(b), it is noticeable that both signals have similar frequency components, which means it would not be suitable to use a low-pass filter to separate them. To be able to use the rotor dynamic information for condition monitoring, however, the gravitational

acceleration should be removed. Two different methods of removing the gravity will be explained in the next section.

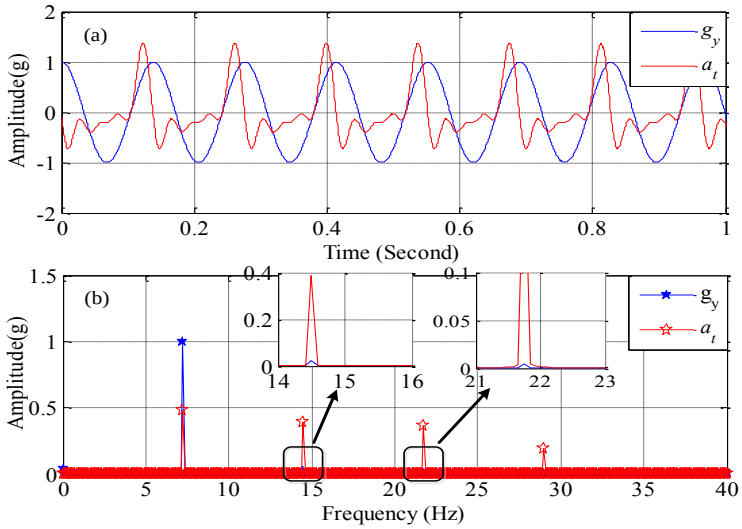

Figure 2: Acceleration signals - (a) tangential acceleration $\tilde{\boldsymbol{a}}_{\boldsymbol{t}}$ and gravitational acceleration projection on Y-axis $\boldsymbol{g}_{\boldsymbol{y}}$ in time domain, and (b) their spectra

2.1 Gravity cancellation using only one on-rotor MEMS accelerometer (one MEMS method)

This method uses only one MEMS accelerometer attached to the compressor flywheel. In this method, as suggested in [7], the gravitational acceleration is removed using both X and Y outputs of a single on-rotor MEMS accelerometer. In [7], it is explained that the gravitational acceleration projection on the Y axis (g_y) is similar to that on the X-axis with a phase shift of $\pi/2$ for all frequency components. Therefore, the gravity can be successfully eliminated, and the real tangential acceleration of interest can be reconstructed by combining the phase-shifted normal and tangential direction outputs of the sensor. The reconstruction steps can be summarised as follows [7]:

1- Remove the high frequency noise by applying a low-pass filter to both $\tilde{a}_x$ and $\tilde{a}_y$ signals;

2- Use the Hilbert transform to add a phase shift of $\pi/2$ to the filtered signal $\tilde{a}_x$;

3- Add the phase-shifted signal to the filtered signal $\tilde{a}_y$, which gives a signal that contains only the tangential acceleration:

$$a_{tx} = \sum_{n=1}^{\infty}(n+2)r\omega_o A_n \cos\left(n\omega_o t+\phi_n\right) \tag{7}$$

4- Scale the amplitude of the nth harmonic component to $n/(n+2)$ in a_{tx} in the frequency domain, and thus obtain the true tangential acceleration a_t. Therefore, the tangential acceleration can be expressed as:

$$a_t = \sum_{n=1}^{\infty} nr\omega_o A_n \cos\left(n\omega_o t+\phi_n\right) \tag{8}$$

where r is the distance from the accelerometer to the wheel centre.

2.2 Gravity cancellation using two MEMS accelerometers (two MEMS method)

As shown in Fig. 3, this method uses two MEMS accelerometers mounted diametrically opposite each other on the reciprocating compressor flywheel, allowing the gravitational acceleration signal to be cancelled by summing the Y-axis signals from both sensors [10].

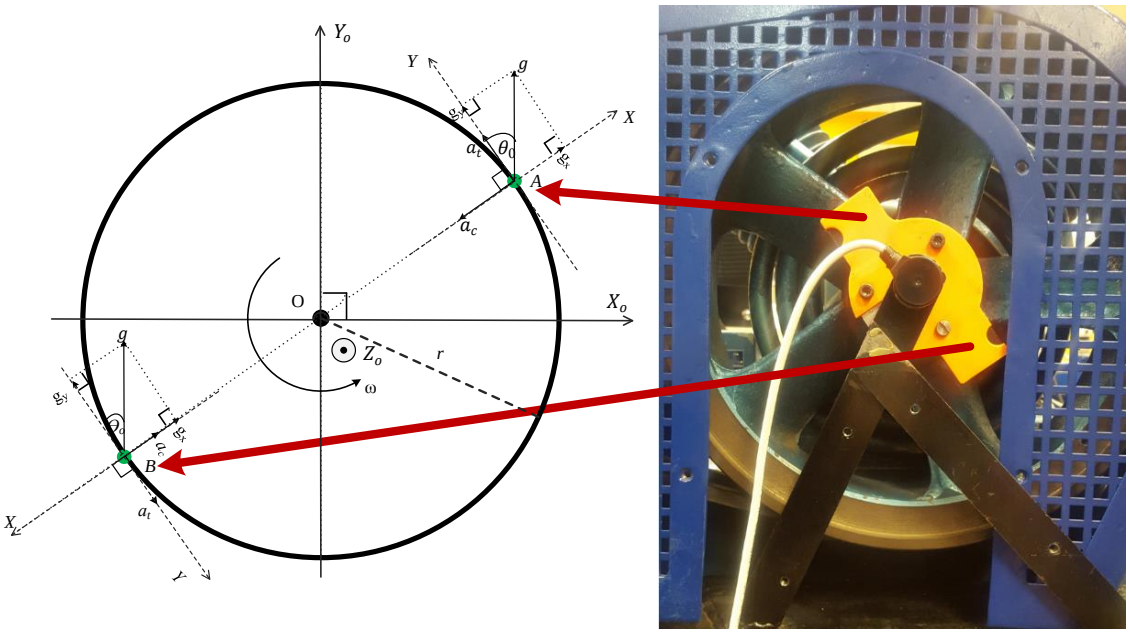

Figure 3: Acceleration analysis of two masses (A and B) rotating around point O

The output signals for sensor A on both the X-axis and Y-axis can be expressed as:

$$\begin{aligned} a_{Ax} &= -a_c + g_x = -a_c + g\sin\theta \\ a_{Ay} &= a_t + g_y = a_t + g\cos\theta \end{aligned} \tag{3}$$

Similarly, for sensor B,

$$\begin{aligned} a_{Bx} &= -a_c - g_x = -a_c - g\sin\theta \\ a_{By} &= a_t - g_y = a_t - g\cos\theta \end{aligned} \tag{4}$$

From Equations 3 and 4, it can be noticed that gravity appears in both the X-axis and Y-axis outputs, but by summing a_{Ay} and a_{By} this undesirable signal can be eliminated and the tangential acceleration can be obtained:

$$a_{Ay} + a_{By} = 2a_t \tag{5}$$

Therefore, the true tangential acceleration can be expressed as:

$$a_t = \frac{a_{Ay} + a_{By}}{2} \tag{6}$$

From Equation 6, it is clear that the real tangential acceleration can be obtained directly just by summing the output signals of the two accelerometers. However, this method has some disadvantages. In the first place, it is not easy to install the MEMS accelerometers in the precise positions; secondly, it is more expensive and thirdly, the sampling rates for the two MEMS sensors might be slightly different, which means more post-processing is required. In this work, both AX3 data loggers were configured to operate with a sampling rate of 1600 Hz. However, when the actual sampling frequencies for these sensors were calculated, they were slightly different from the configured value. The actual sampling frequency for the first sensor was 1590 Hz, while for the other it was 1610 Hz. The sampling rate was corrected using the following process:

1- Synchronise both sensors' data to the same time;
2- Divide both sets of data into many frames;
3- Resample the sensors' data based on the frames.

Supposing that both the first AX3 and the second have independent errors ΔA and ΔB respectively, the total error arising from summing the data from these sensors can be calculated as [11]:

$$TE = \sqrt{(\Delta A)^2 + (\Delta B)^2} \tag{7}$$

where TE denotes the total error of using two MEMS sensors to calculate the tangential acceleration.

3 Experimental work

3.1 Test rig facility

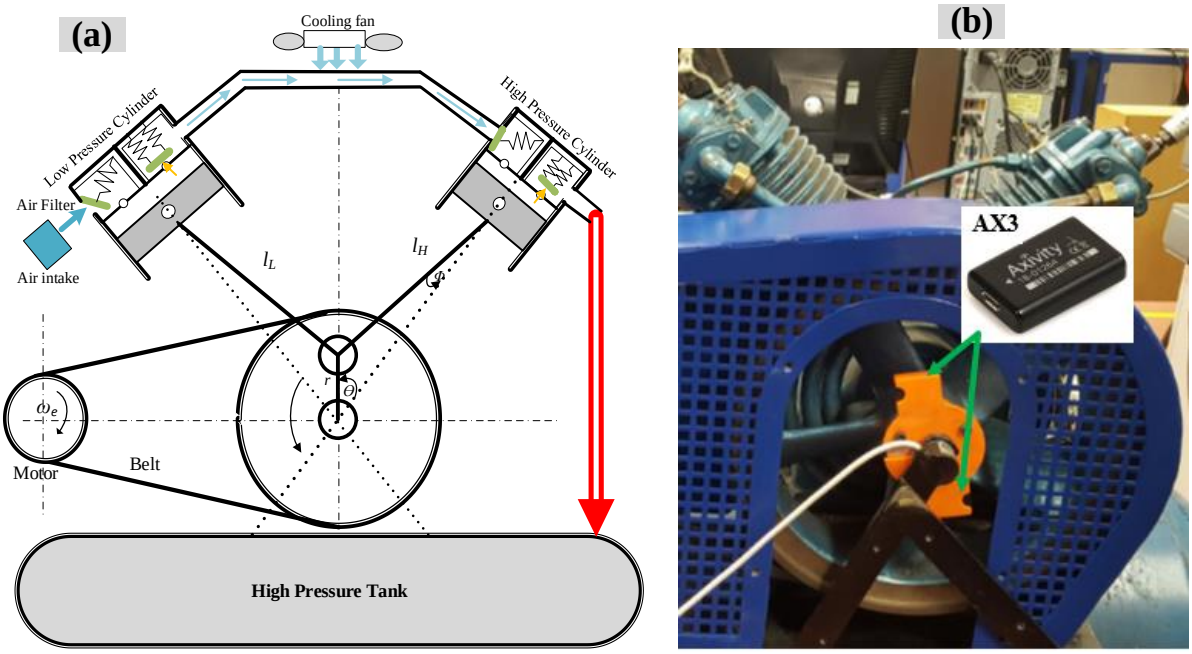

Figure 6: (a) Schematic of a two-stage reciprocating compressor; (b) Installation of MEMS accelerometers on the compressor flywheel

In this experimental work, a reciprocating compressor is used to evaluate the effectiveness of both methods in obtaining true tangential acceleration for condition monitoring. Figure 6(a) shows a diagram of a two-stage reciprocating compressor, which mainly consists of three parts: an electric motor, a compression unit and a high pressure tank to store the compressed air [12]. The compression part is composed of two cylinders, two pistons, two connecting rods, a crankshaft, four self-acting valves and an intercooler.

Two AX3 data logger sensors are mounted diametrically opposite each other on the reciprocating compressor flywheel and close to the centre of the flywheel to record the on-rotor accelerations as illustrated in Figure 6(b). Both data logger sensors are installed 50 mm offset from the centre to allow the full waveform of centripetal acceleration to be within the dynamic range of the data logger. The holders for the MEMS sensors were designed using SolidWorks CAD software, which is one of the best methods for 3D modelling, and printed out using a 3D printer.

3.2 Test procedure

During the test, both AX3 data logger sensors were configured to operate with a dynamic range of ±16g and a sampling rate of 1600 Hz to allow sufficient inspection of the rotor dynamic characteristics [13]. The acquired data were stored in memory during machine run-time, and then exported for post-processing after the machine was shut down. Simultaneously, the tank pressure was also recorded via

a CED 1401 data acquisition system with a sampling rate of 49019 Hz, to act as a load reference for the post-processing.

In this work, two different groups of data have been collected to compare the performance of both methods. The first data are healthy (BL), having been acquired when the system was operating under normal conditions with no faults. The other data have been collected from a system with a leak created in the piping that carries the processing air from the low pressure to high pressure stage; this was simulated by loosening the intercooler by turning the nut through one turn.

4 Results and discussion

Figure 7 shows a typical set of both sensors' outputs in both X and Y axes with their spectra when the compressor operates at around 0.55 MPa (80 psi).

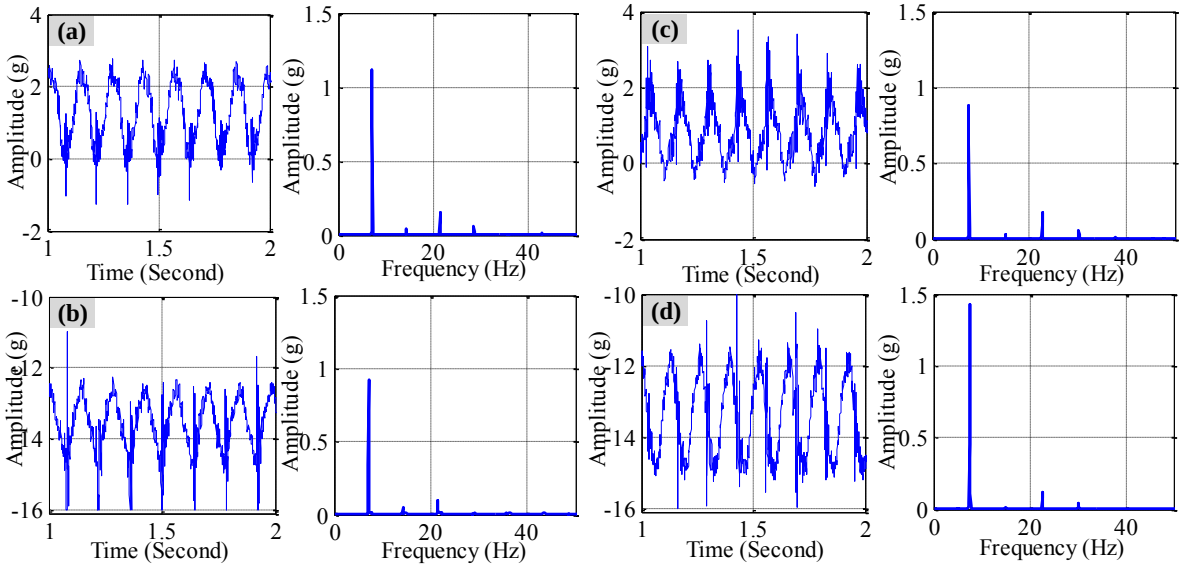

Figure 7: Acceleration signals and their spectra at pressure of 0.55 MPa (80 psi) - (a) X-axis and (b) Y-axis for sensor 1; (c) X-axis and (d) Y-axis for sensor 2

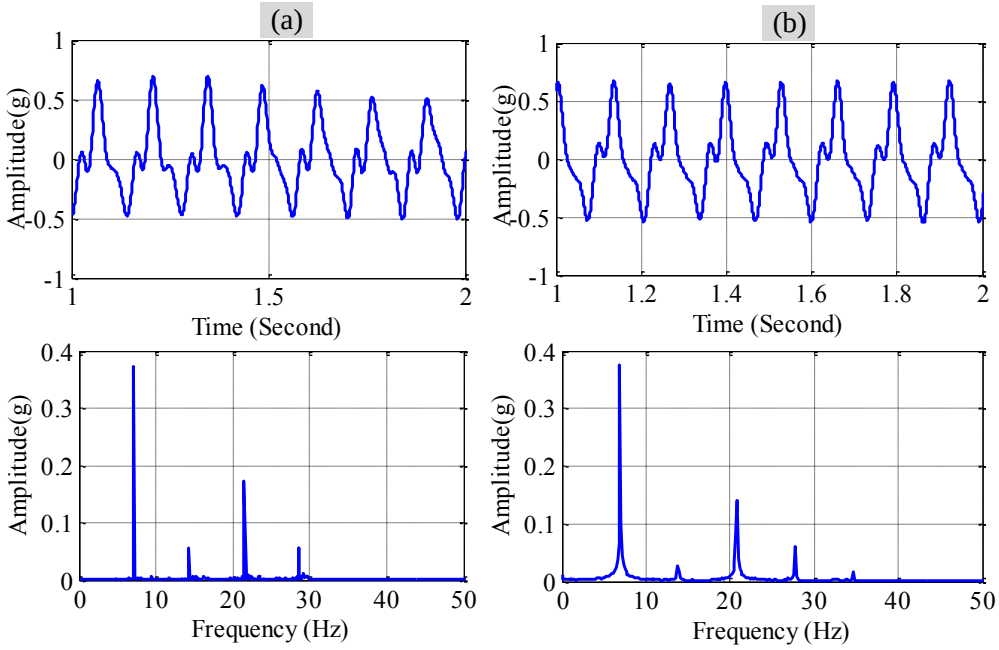

Figure 8: Tangential acceleration signals with tank pressure at 0.55 MPa (80 psi) - (a) One MEMS method (b) Two MEMS method

Figure 8 shows tangential acceleration signals obtained using both methods. It is clear that both signals have a good match in terms of waveform shape, amplitude and frequency components, thus proving the readability of these methods. To demonstrate the classification of compressor conditions using tangential acceleration signals obtained by the methods explained in this paper, the harmonics amplitude changes with tank pressure for two conditions are presented in Figure 9.

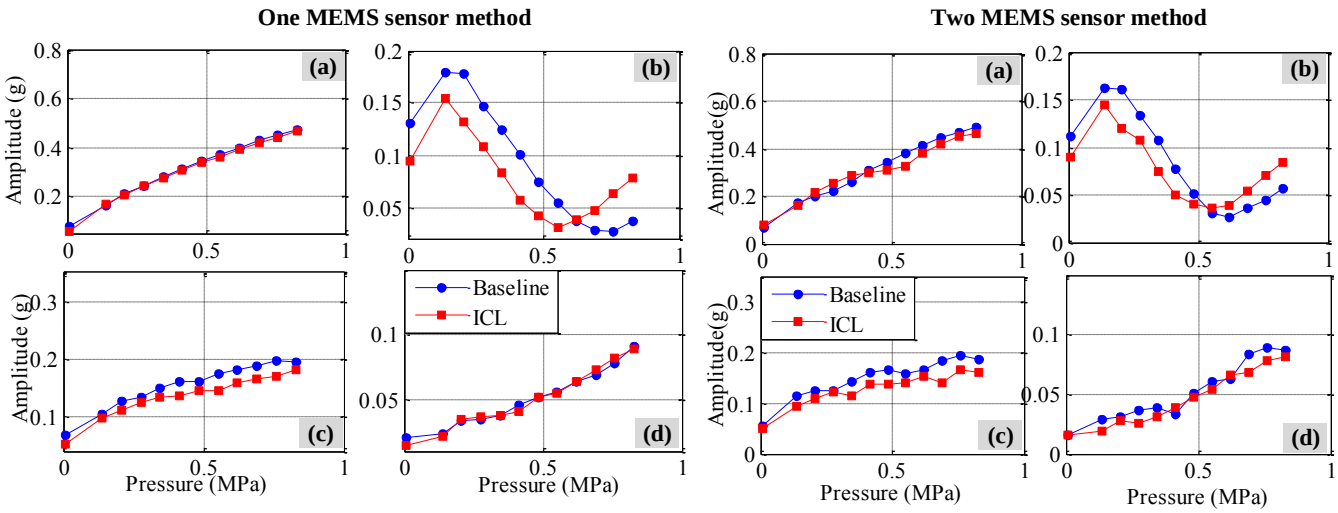

Figure 9: Harmonics amplitude of the reconstructed acceleration signal vs. tank pressure - (a) fundamental frequency, (b) 2nd harmonic, (c) 3rd harmonic and (d) 4th harmonic

From the above figure, it is noticeable that the fundamental and third harmonic amplitudes have a linear increasing trend with tank pressure from 10 to 120 psi, which means that these two components are useful and can be used for further condition classification. Figure 10(a) shows the relationship of the third harmonic with the fundamental frequency for tank pressure ranging from 0.41 MPa to 0.83 MPa (60 psi to 120 psi). Based on the relationship between the fundamental and third harmonic, the intercooler leakage fault signal is classified in Figure 10(b).

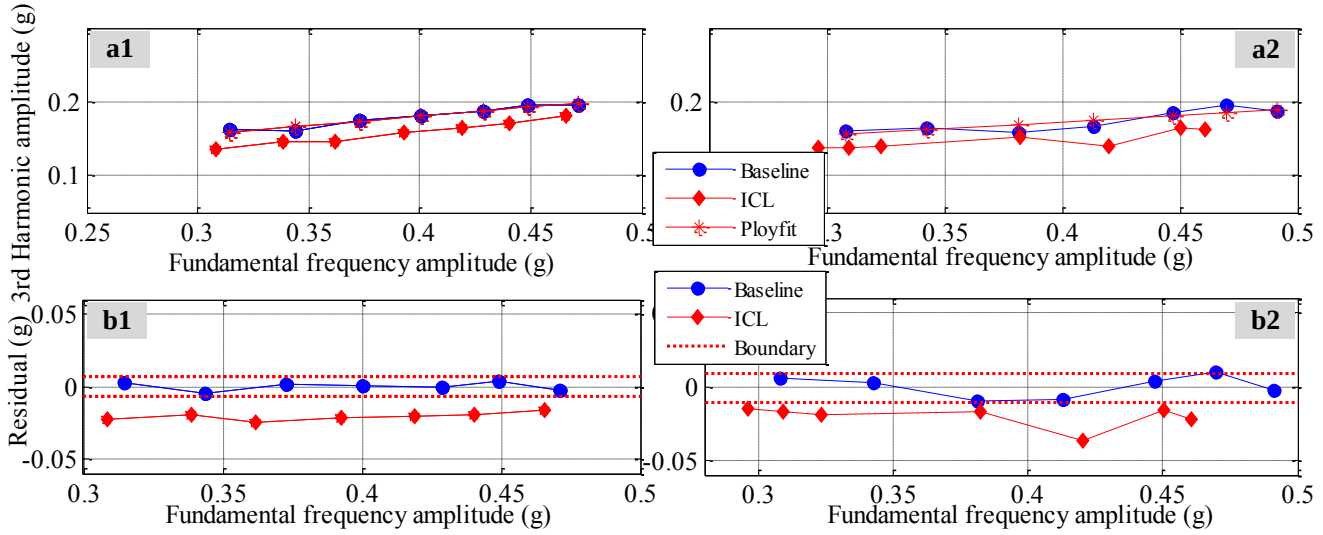

Figure 10: Fault classification - (a1) 3rd harmonic vs. fundamental; (b1) residual vs. fundamental frequency for one MEMS method; (a2) 3rd harmonic vs. fundamental; (b2) residual vs. fundamental frequency for two MEMS method

5 Conclusions

This paper has studied and compared two different methods of removing the gravitational acceleration projection so as to obtain pure tangential acceleration for condition monitoring of

rotating machines. The tangential acceleration signals calculated using both methods have a good match in waveform shape, amplitude and frequency components, and both of them can classify a faulty signal. However, in terms of error analysis, the one MEMS sensor method has a lower error range, which means it has a better performance than the two MEMS sensors method.

REFERENCES

1. Akyildiz, I.F., W. Su, Y. Sankarasubramaniam, and E. Cayirci, *Wireless sensor networks: a survey*. Computer networks, 2002. **38**(4): p. 393-422.
2. Arebi, L., Y. Fan, F. Gu, and A. Ball, *Investigation of wireless sensor deployed on a rotating shaft and its potential for machinery condition monitoring*. 2010.
3. Arebi, L., F. Gu, and A. Ball. *A comparative study of misalignment detection using a novel Wireless Sensor with conventional Wired Sensors*. in *Journal of Physics: Conference Series*. 2012. IOP Publishing.
4. Raj, V.P., K. Natarajan, and S.T. Girikumar. *Induction motor fault detection and diagnosis by vibration analysis using MEMS accelerometer*. in *Emerging Trends in Communication, Control, Signal Processing & Computing Applications (C2SPCA), 2013 International Conference on*. 2013. IEEE.
5. Elnady, M., J.K. Sinha, and S. Oyadiji. *Identification of critical speeds of rotating machines using on-shaft wireless vibration measurement*. in *Journal of Physics: Conference Series*. 2012. IOP Publishing.
6. Thompson, H. *Wireless sensor research at the rolls-royce control and systems university technology centre*. in *Wireless Communication, Vehicular Technology, Information Theory and Aerospace & Electronic Systems Technology, 2009. Wireless VITAE 2009. 1st International Conference on*. 2009. IEEE.
7. Feng, G., N. Hu, Z. Mones, F. Gu, and A.D. Ball, *An investigation of the orthogonal outputs from an on-rotor MEMS accelerometer for reciprocating compressor condition monitoring.* Mechanical Systems and Signal Processing, 2016. **76–77**: p. 228-241.
8. Mones, Z., G. Feng, U.E. Ogbulaor, T. Wang, F. Gu, and A.D. Ball, *Performance evaluation of wireless MEMS accelerometer for reciprocating compressor condition monitoring*, in *Power Engineering*. 2016, CRC Press. p. 893-900.
9. Chaudhury, S.B., M. Sengupta, and K. Mukherjee, *Vibration monitoring of rotating machines using MEMS accelerometer.* International Journal of Scientific Engineering and Research, 2014. **2**(9): p. 11.
10. Baghli, L., J.F. Pautex, and S. Mezani. *Wireless instantaneous torque measurement, application to induction motors*. in *Electrical Machines (ICEM), 2010 XIX International Conference on*. 2010. IEEE.
11. Hildebrand, F.B., *Introduction to numerical analysis*. 1987: Courier Corporation.
12. Elhaj, M., F. Gu, A. Ball, A. Albarbar, M. Al-Qattan, and A. Naid, *Numerical simulation and experimental study of a two-stage reciprocating compressor for condition monitoring.* Mechanical Systems and Signal Processing, 2008. **22**(2): p. 374-389.
13. Axivity, *http://axivity.com/files/resources/AX3_Data_Sheet.pdf*. AX3 Data sheet, 2015.